RESEARCH ARTICLE

Cell Host Response to Infection with Novel Human Coronavirus EMC Predicts Potential Antivirals and Important Differences with SARS Coronavirus

Laurence Josset,[a] Vineet D. Menachery,[b,c] Lisa E. Gralinski,[b,c] Sudhakar Agnihothram,[b,c] Pavel Sova,[a] Victoria S. Carter,[a] Boyd L. Yount,[b,c] Rachel L. Graham,[b,c] Ralph S. Baric,[b,c] Michael G. Katze[a]

Department of Microbiology, School of Medicine, University of Washington, Seattle, Washington, USA[a]; Department of Epidemiology[b] and Department of Microbiology and Immunology,[c] University of North Carolina at Chapel Hill, Chapel Hill, North Carolina, USA

L.J. and V.D.M. contributed equally to this work.

ABSTRACT A novel human coronavirus (HCoV-EMC) was recently identified in the Middle East as the causative agent of a severe acute respiratory syndrome (SARS) resembling the illness caused by SARS coronavirus (SARS-CoV). Although derived from the CoV family, the two viruses are genetically distinct and do not use the same receptor. Here, we investigated whether HCoV-EMC and SARS-CoV induce similar or distinct host responses after infection of a human lung epithelial cell line. HCoV-EMC was able to replicate as efficiently as SARS-CoV in Calu-3 cells and similarly induced minimal transcriptomic changes before 12 h postin-fection. Later in infection, HCoV-EMC induced a massive dysregulation of the host transcriptome, to a much greater extent than SARS-CoV. Both viruses induced a similar activation of pattern recognition receptors and the interleukin 17 (IL-17) pathway, but HCoV-EMC specifically down-regulated the expression of several genes within the antigen presentation pathway, including both type I and II major histocompatibility complex (MHC) genes. This could have an important impact on the ability of the host to mount an adaptive host response. A unique set of 207 genes was dysregulated early and permanently throughout infection with HCoV-EMC, and was used in a computational screen to predict potential antiviral compounds, including kinase inhibitors and glucocorticoids. Overall, HCoV-EMC and SARS-CoV elicit distinct host gene expression responses, which might impact *in vivo* pathogenesis and could orient therapeutic strategies against that emergent virus.

IMPORTANCE Identification of a novel coronavirus causing fatal respiratory infection in humans raises concerns about a possible widespread outbreak of severe respiratory infection similar to the one caused by SARS-CoV. Using a human lung epithelial cell line and global transcriptomic profiling, we identified differences in the host response between HCoV-EMC and SARS-CoV. This enables rapid assessment of viral properties and the ability to anticipate possible differences in human clinical responses to HCoV-EMC and SARS-CoV. We used this information to predict potential effective drugs against HCoV-EMC, a method that could be more generally used to identify candidate therapeutics in future disease outbreaks. These data will help to generate hypotheses and make rapid advancements in characterizing this new virus.

Address correspondence to Michael G. Katze, honey@u.washington.edu.

In September 2012, a novel human coronavirus, HCoV-EMC, was reported to health authorities from two cases of acute respiratory syndrome with renal failure (1–4). The most recent update by the WHO identified a total of 17 confirmed cases of human infection, including 11 deaths, suggesting a mortality rate of ~65% (5). All of these individuals had a history of recent travel to the Middle East. Identification of clusters of coronavirus cases indicates that HCoV-EMC can be transmitted from human to human (6) and raises concern about a possible outbreak of this virus, similar to the one caused by a related virus, the severe acute respiratory syndrome-related coronavirus (SARS-CoV), in 2002–2003. SARS-CoV, originating in China, spread throughout Asia and to other continents and affected more than 8,000 people (7, 8). The overall mortality during the outbreak was estimated at 9.6% (7).

While the mortality rate of HCoV-EMC cannot be assessed with certainly, it could be more pathogenic than SARS-CoV.

HCoV-EMC belongs to the genus betacoronavirus, as does SARS-CoV. However, HCoV-EMC is more closely related to the bat coronaviruses HKU4 and HKU5 (lineage 2C) than it is to SARS-CoV (lineage 2B) (2, 9). Less than 50% amino acid sequence identity is conserved in the replicase domains between SARS-CoV and HCoV-EMC. Another important difference between the two viruses is that they do not use the same host cell receptor for infection (10). Indeed, it was clearly shown that human angiotensin-converting receptor 2 (hACE2), used by SARS-CoV, is not the HCoV-EMC receptor (10). Dipeptidyl peptidase 4 was recently identified as the HCoV-EMC receptor (11). This receptor is conserved among different species such as bats and humans,

partially explaining the large host range of HCoV-EMC. This was somewhat surprising, as coronaviruses generally show strict host specificity.

While recent identification of the crystal structure of HCoV-EMC protease suggests that a wide-spectrum CoV protease inhibitor could block the catalytic site (12), there is currently no proven antiviral treatment for HCoV-EMC. Viruses rely on host factors to replicate and often hijack cellular processes initiated in response to infection to ensure efficient replication (13). Targeting cellular responses has been shown to inhibit viral replication (13, 14). Furthermore, immunomodulatory drugs that reduce the excessive host inflammatory response to respiratory viruses, as seen with influenza virus infections, have therapeutic benefit (reviewed in reference 15). Several genome-based drug repurposing strategies successfully identified known drugs that could be reused to treat lung cancer, inflammatory bowel disease (16), and influenza virus infection (14). Such an approach has the advantage of accelerating treatment availability, which could be crucial in case of an outbreak of an emerging pathogen.

Overall, differences in viral sequences, host cell receptor, and host range indicate that HCoV-EMC and SARS-CoV may have distinct strategies for interacting with their hosts. This fact could impact treatment strategies. To begin to assess this question, we compared the host response of human cells to HCoV-EMC and SARS-CoV infection using global transcriptomic profiling. Our goal was to gain a rapid and comprehensive assessment of the host response to HCoV-EMC infection that could guide research on this emerging virus. Importantly, we used this information to computationally predict antiviral treatment and identified a broad down-regulation of the antigen presentation pathway that may be important *in vivo* for the development of an adaptive immune response.

RESULTS

SARS-CoV and HCoV-EMC have similar replication kinetics but different cytopathic effects in a human epithelial cell line. To characterize HCoV-EMC, we sought a cell line that mimics the human airway. Calu-3 cells, derived from epithelial cells lining the human conducting airway, can be differentiated into polarized ciliated cells and permit robust replication of several respiratory viruses, including SARS-CoV, influenza A virus, and respiratory syncytial virus (RSV) (17–20). Therefore, Calu-3 cells were infected with HCoV-EMC using a multiplicity of infection (MOI) of 5, and results were compared with those for Calu-3 cells infected with SARS-CoV Urbani at the same MOI. The viruses replicated to similar levels, with both peaking at >10^7 PFU at 24 h postinfection (hpi) (Fig. 1). While SARS-CoV has been previously shown to maintain steady replication and cell viability to 72 hpi (19), HCoV-EMC induced substantial cytopathic effect at 18 to 24 hpi, with significant cell rounding and detaching. Together, these data suggest that although HCoV-EMC and SARS-CoV exhibit similar replication kinetics, they elicit different host responses in lung epithelial cells.

HCoV-EMC induces earlier and different transcriptional changes than SARS-CoV. To assess the global host transcriptional response following infection with HCoV-EMC, samples of infected Calu-3 cells were collected throughout a 24-h time course postinfection. Genes that were differentially expressed (DE) compared to time-matched mock-infected controls were determined using the statistical cutoff of a *q* value of <0.01 and an absolute
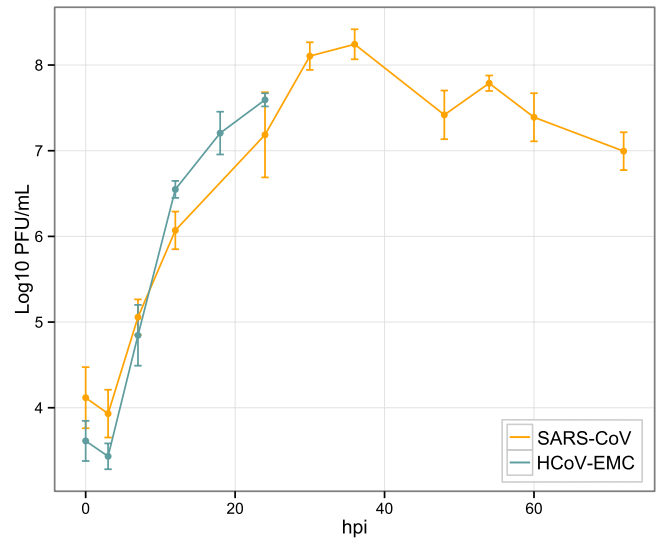

FIG 1 HCoV-EMC replicates at a level similar to that of SARS-CoV in human epithelial cells. Triplicate wells of Calu-3 2B4 cells were infected with HCoV-EMC (MOI, 5). Medium from each well was collected and analyzed by plaque assay for viral growth kinetics in VeroE6 cells. The corresponding cells were harvested for transcriptomic analysis. SARS-CoV titers after infection of Calu-3 2B4 cells at an MOI of 5 were determined using the same method (19). The error bars represent the standard deviations among triplicate cell samples.

$\log_2$(FC) of >1. These genes were compared to DE genes from Calu-3 cells infected with SARS-CoV across a 72-h time course using the same statistical cutoff (Fig. 2).

As previously observed (19), SARS-CoV is able to replicate actively with a surprisingly small number of significant transcriptional changes before 24 hpi (from 5 DE genes at 0 hpi to 47 genes at 12 hpi) (Fig. 2A). Similarly, HCoV-EMC induced fewer transcriptional changes before 12 hpi than after. However, HCoV-EMC replication at early times postinfection induced more changes than SARS-CoV, with the number of DE genes ranging from 28 at 0 hpi to 206 genes at 12 hpi (Fig. 2A). At later times postinfection, a massive host response was observed during HCoV-EMC infection, with 6,532 DE genes at 18 hpi and 11,664 genes at 24 hpi, while SARS-CoV induced changes of only 792 genes at 24 hpi with maximum changes at 48 and 54 hpi of 6,496 and 6,498 genes, respectively.

To evaluate the similarity of transcriptional dysregulation between HCoV-EMC and SARS-CoV, we determined the percentage of overlap among DE genes changing in the *same* direction at each time point (Fig. 2B). The intersection between up- or down-regulated DE genes for each condition was calculated separately and then averaged to determine the percentage of intersecting genes (Fig. 2B). The overlap between signatures at late times postinfection for a single virus was very high; for example, 89% of the genes DE by HCoV-EMC at 18 hpi were also DE at 24 hpi, and on average 77% of the DE genes at 24 hpi with SARS-CoV were also DE at later times postinfection. However, the overlap between SARS-CoV and HCoV-EMC at the same time point was low; for example, only 3% of the DE genes in response to HCoV-EMC at 24 hpi were also DE by SARS-CoV at this time point. Of note, the intersection of DE genes between the two infections was higher when later times postinfection for SARS-CoV were compared with earlier time points for HCoV-EMC. On average 22% of the
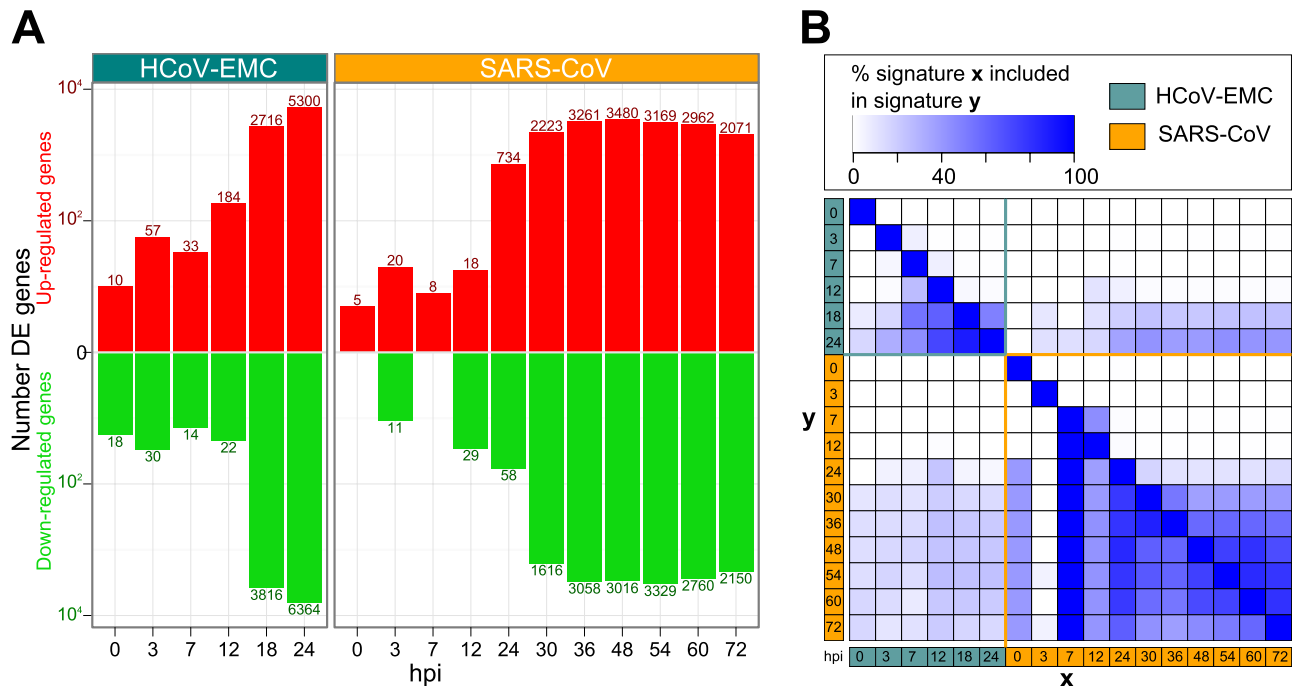
FIG 2 HCoV-EMC induces more and different transcriptional changes than SARS-CoV at similar times postinfection. (A) Number of up-regulated (red) and down-regulated (green) differentially expressed (DE) genes after infection with HCoV-EMC and SARS-CoV compared to time-matched mock-infected controls. The criterion used for differential expression analysis is a q value of <0.01 as determined by Limma's empirical Bayes moderated t test and a $|\log_2 FC|$ of >1. (B) Percentage of DE genes under the condition shown on the x axis that intersect with DE genes under the condition shown on the y axis. To identify overlap among genes changing in the same direction, up- and down-regulated signatures are intersected separately, and the average of the two percentages is shown by a white-to-blue gradient (0% to 100%).

HCoV-EMC signatures from 12 to 24 hpi overlapped the signatures of SARS-CoV from 36 to 72 hpi. Together, these results indicate that HCoV-EMC induced both a more robust and a largely different host response compared to that induced by SARS-CoV at similar times postinfection. However, changes induced from 12 to 24 hpi after HCoV-EMC were more similar to changes induced late after SARS-CoV infection (24 to 72 hpi).

HCoV-EMC massively dysregulates the host transcriptome at late times postinfection. At late times postinfection, HCoV-EMC induced drastic changes in the host transcriptome with 12,392 DE genes at 18 hpi and/or 24 hpi. To characterize this late signature, we compared the $\log_2$ fold change ($\log_2$ FC) expression values of these 12,392 genes after infection with SARS-CoV or HCoV-EMC (Fig. 3 and www.systemsvirology.org). There were 3,474 genes (28%) expressed similarly to those in SARS-CoV-infected samples at the same or later times postinfection and 8,918 genes (72%) expressed differently than during SARS-CoV infection. These genes were further clustered according to their expression pattern in HCoV-EMC infected cells (clusters I and III contain genes up-regulated after HCoV-EMC infection at 18 to 24 hpi; clusters II and IV contain down-regulated genes). Enrichment in canonical pathways for each of this cluster was performed and is shown Fig. 3B.

Genes that were up-regulated by both HCoV-EMC and SARS-CoV (cluster I), though later by SARS-CoV than by HCoV-EMC, were primarily related to viral recognition and the activation of innate immune pathways: the IL-17-related pathway and activation of interferon regulatory factor (IRF) by cytosolic pattern recognition receptors. Genes down-regulated by both viruses (cluster II) were related to metabolism.

Genes specifically up-regulated by HCoV-EMC were statistically enriched in only 2 pathways: cAMP-mediated signaling and protein ubiquitination. Because ubiquitination is involved in the innate immune antiviral response (21), this could represent an interesting mechanism to explore further. Finally, genes specifically down-regulated after HCoV-EMC infection were largely related to the antigen presentation pathway. In addition, the other identified canonical pathways are strongly related to lymphocyte signaling processes. Together, these data suggest that HCoV-EMC may quickly move to interfere with elements of the adaptive immune response, in contrast to SARS-CoV.

The antigen presentation pathway is broadly down-regulated after HCoV-EMC infection. As down-regulation of the antigen presentation pathway may have important implications for the development of the adaptive response, we more closely examined changes in this pathway after infection with HCoV-EMC (Fig. 4). Twenty-two genes related to major histocompatibility complex (MHC) class I, MHC class II, or antigen presentation were found to be down-regulated after HCoV-EMC infection (Fig. 4A), while in contrast, the vast majority of these genes were up-regulated by SARS-CoV infection after 36 hpi (Fig. 4B). Interestingly, transcriptional regulators of MHC class I (*NLRC5*) and MHC class II (*CIITA*) were transiently up-regulated early after HCoV-EMC infection (at 12 and 0 hpi, respectively). Other genes were down-regulated starting at 12 hpi. Importantly, both MHC class I genes (*HLA-A*, *-B*, *-C*, *-E*, and *-G*) and class II genes (*HLA-DMB*, *-DPA1*, *-DPB1*, *-DQA1*, *-DRA*, *-DRB1*, *-DRB3*, *-DRB4*, and *-DRB5*) had decreased expression values after infection. Several genes from the MHC I pathway, including proteasome genes (*PSMB8* and *PSMB9*), genes from the peptide-loading complex
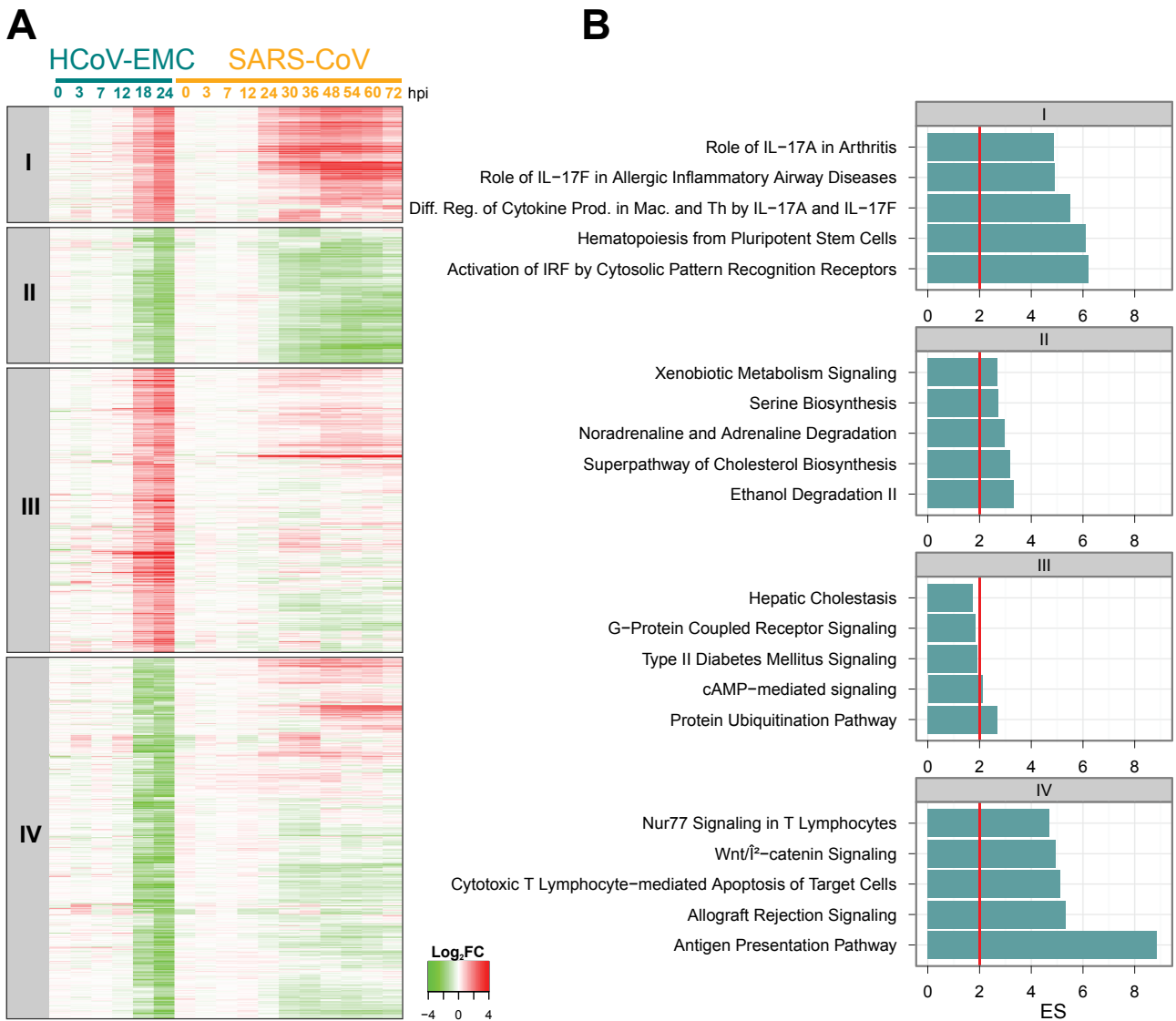
FIG 3 HCoV-EMC massively dysregulates the host transcriptome at late times postinfection and triggers both similar and unique pathways compared to those induced by SARS-CoV. (A) Heatmap depicting the expression values of 12,392 genes DE after infection with HCoV-EMC at late times postinfection (union of DE genes at 18 and 24 hpi). Genes were clustered into four main sets: set I includes 1,599 genes that are significantly up-regulated after infection with both HCoV-EMC and SARS-CoV; set II includes 1,875 genes that are significantly down-regulated after infection with both HCoV-EMC and SARS-CoV; set III includes 3,922 genes that are significantly up-regulated after infection with HCoV-EMC but not DE with SARS-CoV; and set IV includes 4,996 genes that are significantly down-regulated after infection with HCoV-EMC but not DE with SARS-CoV. (B) For each of the four clusters, the top 5 enriched canonical pathways are reported. Enrichment score (ES) was defined as $-\log_{10}(P\ \text{value})$ of enrichment. Red lines depict the limit of significance ($P < 0.01$).

(*PDIA3* and *TAPBP*), and *B2M*, were down-regulated, as well as the gene for the invariant chain (*CD74*), which belongs to the MHC II pathway. Down-regulation of genes within MHC I and II pathways was confirmed by quantitative reverse transcription-PCR (RT-PCR), with all 9 genes tested having significantly decreased expression in HCoV-EMC samples (Fig. 4C). Together, the data show that HCoV-EMC and SARS-CoV induce opposite regulation of the entire antigen presentation pathway.

Early and sustained transcriptional changes may be reverted by kinase inhibitors and glucocorticoids. With the goal of identifying possible drugs that will modulate the host response throughout infection and from early times postinfection, we focused on characterizing the early transcriptional changes induced by HCoV-EMC that remained stable throughout the infection. Among the 348 genes DE early after infection (at 0, 3, 7, and/or 12 hpi), 207 (59%) remained dysregulated, with the same pattern at later times postinfection. We chose to focus on this 207-gene signature to avoid transient events that were specific to one time postinfection and to exclude genes with inconsistent expression patterns across the course of infection. Expression values for these genes are displayed in Fig. 5A and are available at www.systems virology.org. This early signature was enriched in genes related to the inflammatory response with IL-17, tumor necrosis factor 2 (TNFR2)-related pathways, and predicted activation of chemotaxis of leukocytes (see Table S1 in the supplemental material). None of the 207 genes were DE early after SARS-CoV infection;
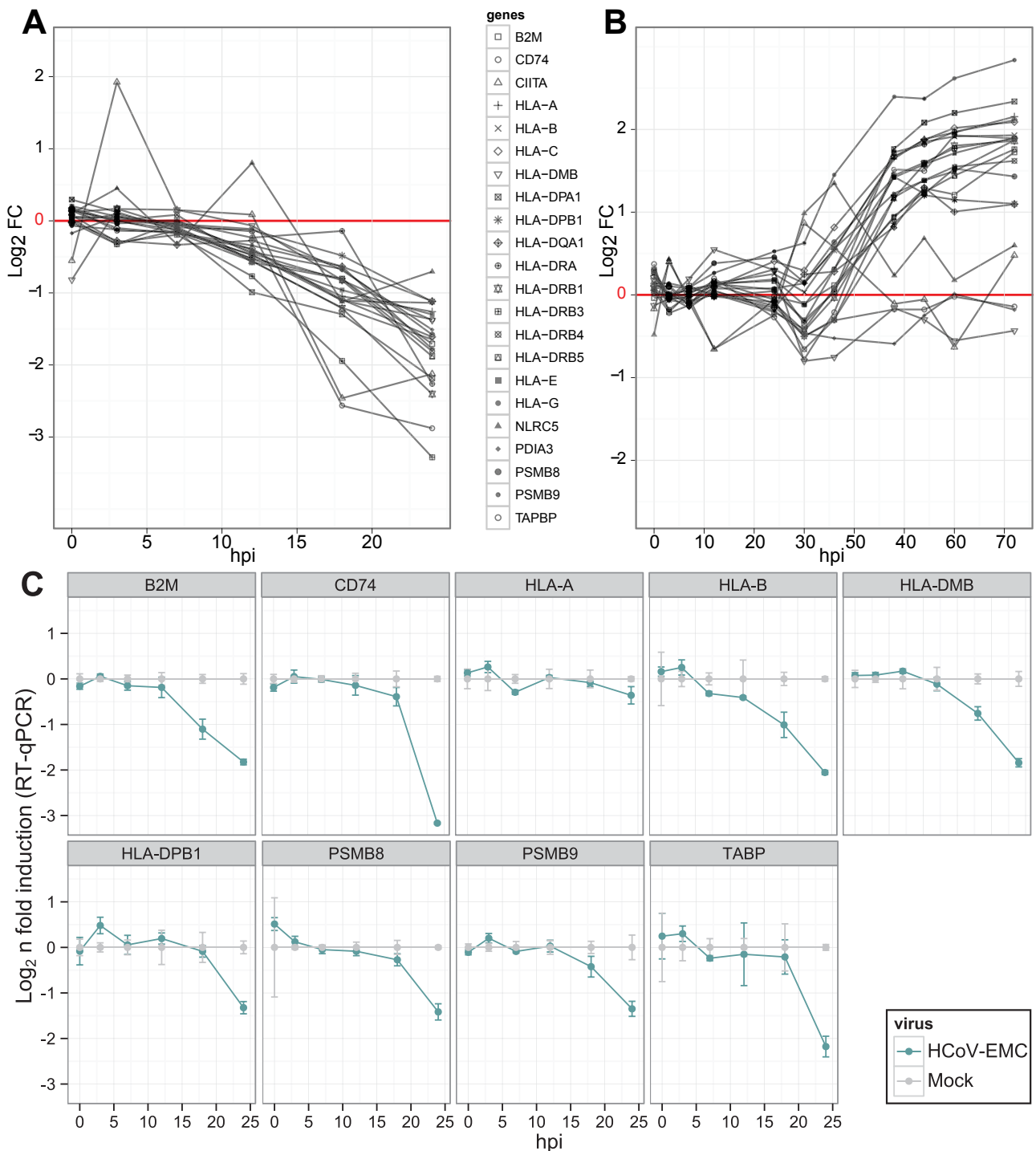
FIG 4 The antigen presentation pathway is specifically down-regulated after infection with HCoV-EMC. (A) Temporal gene expression changes of the 22 genes belonging to the antigen presentation pathway specifically down-regulated after HCoV-EMC infection. (B) Temporal changes for the same set of genes after SARS-CoV infection. Note that the time scale and log $_2$ FC ranges are not the same in panels A and B. (C) Quantitative RT-PCR measurement of the antigen presentation pathway genes expression following HCoV-EMC infection.

however, expression of 51 genes (24.5%) was changed after 24 hpi. This subset of 51 genes was enriched in cell viability molecules, glucocorticoid receptor signaling, and IL-17-related pathways.

In an effort to identify potential drugs that could block the host response to HCoV-EMC, we used the early 207-gene signature and IPA (Ingenuity pathway analysis) upstream regulator analysis (see Materials and Methods) to identify the upstream regulators that may be responsible for gene expression changes observed early after infection. Upstream regulators are defined as any molecule that can affect the expression of another molecule, including
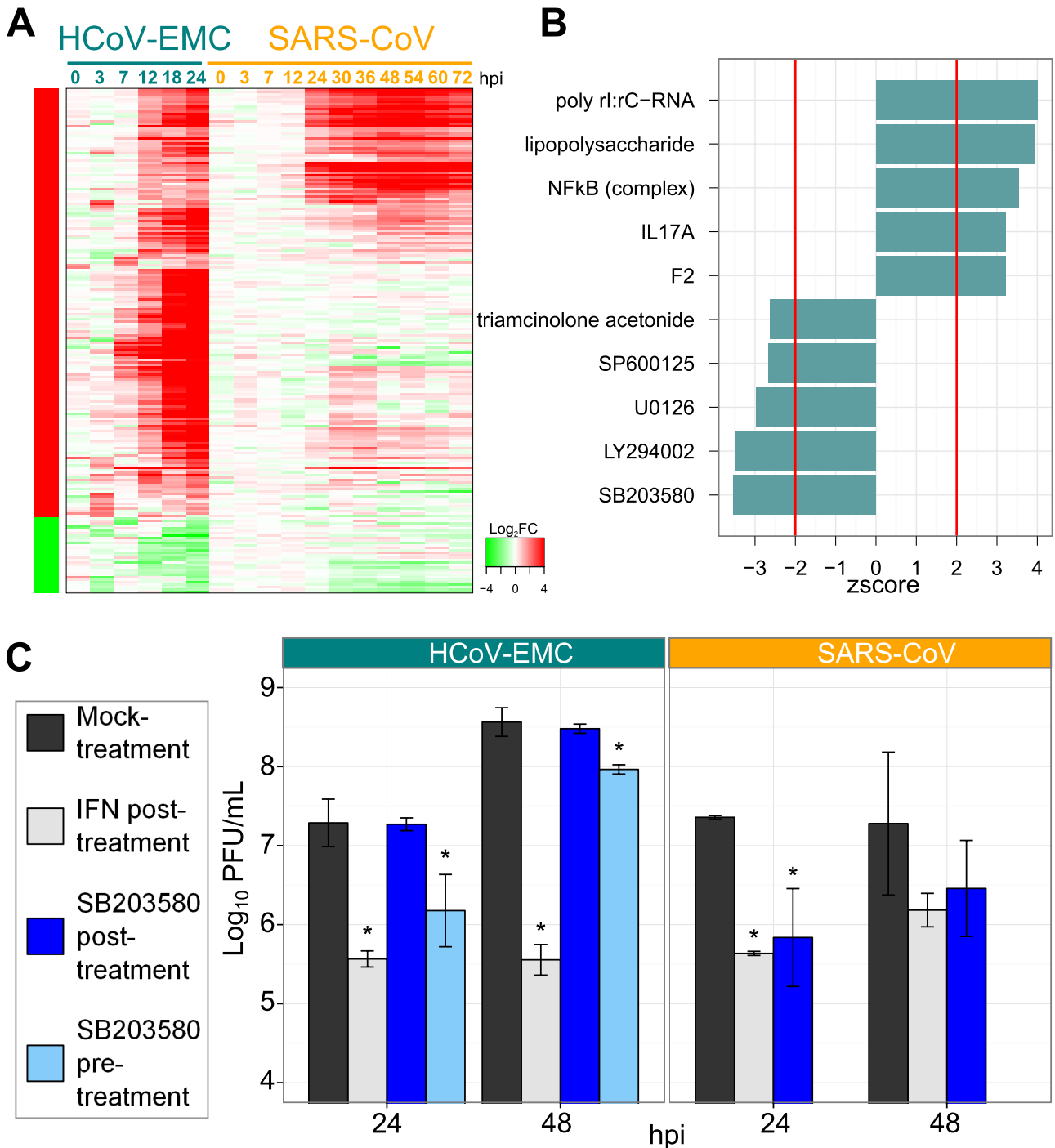
FIG 5 Expression values and major upstream regulators for the 207 genes dysregulated early and constantly after infection with HCoV-EMC. (A) Heatmap depicting the expression values of 207 genes whose expression changed early after infection with HCoV-EMC (at 0, 3, 7, and/or 12 hpi) and remained up- or down-regulated later in infection (18 and 24 hpi). The color key on the left indicates the direction of changes across infection, with red depicting genes significantly up-regulated at at least one time postinfection and green showing genes significantly down-regulated. Genes were clustered based on their expression values across samples using Pearson correlation and complete linkage function. (B) Top 5 activated upstream regulators and top 5 inhibited upstream regulators of the early signature. The prediction of activation state is based on the global direction of changes of the 207 genes throughout infection with HCoV-EMC. Red lines depict the limit of significance ($|z$ score$| > 2$). (C) Analysis of HCoV-EMC and SARS-CoV replication following SB203580 pre- or posttreatment (5 μM). IFN-α posttreatment was used as a reference. *, $P < 0.01$ (Student's t test).

transcription factors, cytokines, micro-RNAs and drugs. The activation state for each regulator was predicted based on global direction of changes throughout infection for previously published targets of this regulator. The predicted top five activated and top five down-regulated regulators are shown in Fig. 5B. The top five activated upstream regulators included genes and mole-

cules that are known to induce the activation of inflammatory genes that were also found up-regulated in the early signature. The top predicted inhibited regulators included four kinase inhibitors (SB203580, LY294002, U0126, and SP600125) and one corticosteroid (triamcinolone acetonide). These molecules are known to down-regulate the same genes that were up-regulated early and across HCoV-EMC infection. In addition, several kinase inhibitors (including SB203580, LY294002, and U0126) and a glucocorticoid (dexamethasone) were also predicted to be negative regulators of genes changed similarly after SARS-CoV and HCoV-EMC infection at late times postinfection (see Table S2 in the supplemental material). Therefore, we hypothesize that treating cells with these drugs might partially revert CoV signatures and inhibit deleterious host responses and/or viral replication in the case of both SARS-CoV and HCoV-EMC.

In silico and in vitro evidence for kinase inhibitors as potential anti-CoV. To test these hypotheses, we first analyzed whether cells treated with identified kinase inhibitors have gene expression profiles opposite to the one induced after viral infection. To this end, we used Connectivity Map (cmap), which is a database of more than 1,309 drug transcriptional signatures in several cell lines (22). This data-driven tool allows the identification of molecules that induce similar or opposite transcriptional changes relative to the query signature, based on their connectivity scores. The connectivity score is a value between $+1$ and -1, where a high positive score indicates that the drug induces changes similar to those induced by viral infection, while a high negative score indicates that the drug reverses the expression of the HCoV-EMC signature. Cmap includes transcriptional profiles of several kinase inhibitors, including two compounds that were predicted to be potential negative regulators of viral response in IPA upstream regulator analysis (SB203580 and LY294002). SB203580 had a connectivity score of -0.733 in MCF7 cells (Data set S1 in the supplemental material), and LY294002 had negative scores in 4 of the 5 cell lines tested in cmap (-0.281 in HL60, -0.146 in MCF7, -0.252 in PC3, and -0.811 in SKMEL5), indicating that these two drugs reversed the expression profile of HCoV-EMC signature. Other related kinase inhibitors present in cmap are U0125 (a derivative of U0126) and SB202190, which both had negative scores in PC3 cells (-0.649 and -0.406, respectively).

To further validate the potential effectiveness of identified kinase inhibitors, we evaluated the ability of the top predicted negative upstream regulator, SB203580, to interfere with viral replication (Fig. 5C). Importantly, this kinase inhibitor was predicted to regulate genes that were DE similarly by SARS-CoV and HCoV-EMC at late times postinfection (see Table S2 in the supplemental material) and could therefore inhibit both viruses' replication. Treating cells with 5 μM SB203580 following SARS-CoV infection resulted in a significant decrease of 20% in the $\log_{10}$ viral titer at 24 hpi ($P < 0.01$); these replication levels are similar to those in interferon (IFN)-treated cells. SB203580 was less effective against EMC-CoV, showing no efficacy with posttreatment; however, pretreatment of infection resulted in significant decreases of 15% and 7% of the $\log_{10}$ viral titer, at 24 and 48 hpi, respectively ($P < 0.01$). Efficacy against SARS-CoV can be explained by the fact that all genes that were DE after SARS-CoV infection were predicted to be regulated by kinase inhibitors (cluster I and II genes [Fig. 3] and additional genes specific to SARS-CoV [data not shown]), while the 8,918 genes specific to HCoV-EMC (clusters III and IV [Fig. 3]) did not include any kinase inhibitor in their upstream

negative regulators (see Table S2). In addition, host response dynamics to SARS-CoV and HCoV-EMC were different, with a delayed and more limited response to SARS-CoV allowing SB203580 posttreatment to be effective. In contrast, EMC-CoV rapidly induced host expression changes and thus required SB203580 pretreatment for measurable effect. As genes specific to HCoV-EMC were predicted to be negatively regulated by other classes of molecules (like gemfibrozil, which targets PPARα; $z = 2.96$), it will be important to determine whether using such molecules in combination with kinase inhibitors like SB203580 could provide a better inhibition of viral replication. Together, these data demonstrate the efficacy of SB203580 against two unique CoVs and validate *in silico* approaches to predict effective drug treatment for emergent viruses.

DISCUSSION

HCoV-EMC was isolated from a patient who died from an acute respiratory disease similar to that caused by SARS-CoV. However, there are several indicators that the host responses to these two viruses may be significantly different. Several cases of HCoV-EMC infection have resulted in renal failure, which has rarely been observed in SARS-CoV infection. In addition, SARS-CoV and HCoV-EMC do not use the same cell receptor, and there are important differences in their genomic sequences. This study adds strength to the assertion that "HCoV-EMC is not the same as SARS-CoV" (23). Indeed, even though we identified specific characteristics of the SARS-CoV response in the HCoV-EMC signatures, HCoV-EMC induced robust and specific transcriptional responses that were distinct from those induced by SARS-CoV, including the broad down-regulation of MHC molecules.

This study is the first global transcriptomic analysis of the cellular response to HCoV-EMC infection. Kindler et al. performed RNA-Seq on human airway epithelium (HAE) cells infected with HCoV-EMC (24). However, their analysis was focused on viral sequences and did not include a genome-wide analysis of the host response. They did, however, use RT-qPCR (quantitative PCR) to compare expression levels of a set of 15 genes, including IFN, RNA sensor molecules, and IFN-stimulated genes (ISGs), following infection with HCoV-EMC, SARS-CoV, or HCoV-229E (MOI 0.1). In our study, we confirm that SARS-CoV and HCoV-EMC induce a similar up-regulation of RNA sensor molecules, such as *RIGI*, *MDA5*, and two of three genes of ISGF3 (*IRF9* and *STAT1*) (genes in cluster I [Fig. 3]). Of note, HCoV-EMC titers were up to 10^2-fold higher than those of SARS-CoV in HAE cells (24), whereas we observed similar viral replication of the two CoVs in Calu-3 cells. Lower replication of SARS-CoV in HAE cells might be explained by the mixed cell population in these primary cultures, with likely nonuniform expression of SARS-CoV receptor (*ACE2*). In contrast, Calu-3 2B4 cells used in our study are a clonal population of Calu-3 cells sorted for ACE2 expression which support high replication of SARS-CoV. In addition, while Kindler et al. noted the absence of induction of *IFN-β* at 3, 6, and 12 hpi (24), we found a specific up-regulation of *IFN-α5* and *IFN-β1* by HCoV-EMC at 18 and 24 hpi (genes in cluster III) and an up-regulation of *IFN-α21* by both SARS-CoV and HCoV-EMC at 24 hpi (cluster I) (expression values for all DE genes are available at http://www.systemsvirology.org). These data illustrate that HCoV-EMC and SARS-CoV both trigger the activation of pattern recognition receptors but may subsequently induce different levels of IFN. Moreover, there were stark differences in global downstream ISG

expression following infection with SARS-CoV or HCoV-EMC; this analysis is discussed in detail elsewhere (V. D. Menachery et al., submitted for publication).

Activation of similar innate viral-sensing pathways by HCoV-EMC and SARS-CoV is not surprising given the conservation of this mechanism to detect foreign RNA and familial relationships of the viruses. We also found that both viruses induced proinflammatory cytokines related to IL-17 pathways. It has previously been shown that IL-17A-related gene expression exacerbates severe respiratory syncytial virus (RSV) or influenza virus infection (25, 26). IL-17A was predicted to be activated throughout infection with HCoV-EMC and may induce immune-mediated pathology that possibly contributes to a high mortality rate. IL-17A is known to be produced by T-helper cells, but its expression in Calu3 cells was increased up to 2-fold at 24 hpi after HCoV-EMC infection. Interestingly, IL-17C and IL-17F, which can be produced by epithelial cells under certain inflammatory conditions and which activate pathways similar to IL-17A-mediated responses (27), were increased earlier and to a greater extent following HCoV-EMC infection (up to 3-fold at 18 hpi for IL-17C and 4-fold at 7 hpi for IL-17F). Therefore, further study of the IL-17 response may provide interesting targets to limit lung injury (26).

A main difference between responses to HCoV-EMC and SARS-CoV was the specific down-regulation of the antigen presentation pathway after HCoV-EMC infection. In contrast, these genes were found to be up-regulated after SARS-CoV infection. Several viruses have evolved mechanisms to inhibit both the MHC class I (reviewed in references 28 and 29) and class II (reviewed in reference 30) pathways. While expression of MHC class II is usually limited to professional antigen-presenting cells, human lung epithelial cells constitutively express this complex (31). Our data demonstrated down-regulation of the MHC class II transactivator (*CIITA*) after HCoV-EMC infection, a finding that possibly explains decreases in MHC class II molecule expression; this is a common viral strategy used to block that pathway (30). MHC class II inhibition can prevent class II-mediated presentation of endogenous viral antigens produced within infected cells and impair the adaptive immune response. Similarly, MHC class I genes were also down-regulated after HCoV-EMC infection; decreasing expression of MHC class I can attenuate CD8 T-cell-mediated recognition of infected cells and could allow immune evasion by HCoV-EMC. Finally, *PSMB8* and *PSMB9*, parts of the immunoproteasome, were also down-regulated by HCoV-EMC; these components replace portions of the standard proteasome and enhance production of MHC class I binding peptides (32). In their absence, proteins targeted for degradation may not generate peptides that robustly bind MHC class I, thus limiting their presentation. Down-regulation of *PSMB8* and *PSMB9* could counteract the host response to viral infection, including up-regulation of ubiquitins and ubiquitin ligases observed during HCoV-EMC infection (Fig. 3B) that may ineffectively target viral protein for degradation. Together, the inhibition of MHC class I and II as well as immunoproteasome construction may have an important impact on the *in vivo* adaptive immune response against HCoV-EMC.

While there is no proven effective antiviral therapy against SARS-CoV (33), several molecules have *in vitro* antiviral activity, including ribavirin, lopinavir, and type I IFN, but their benefits for patients are unclear (33). IFN-α pretreatment of cells has been shown to inhibit HCoV-EMC replication (24), but no direct antiviral therapies have been reported. Targeting host factors impor-

tant for the virus, instead of the virus itself, has been investigated for HIV (34) and influenza virus (13). For example, inhibiting upstream regulators (such as NF-κB) that control the host response to influenza virus infection has been shown to reduce virus replication *in vitro* and in mice (35). Inhibition of immunophilins that interact with the viral nonstructural protein 1 (Nsp1) resulted in potent inhibition of SARS-CoV replication (36, 37). In this study, we characterized upstream regulators predicted to be activated (e.g., NF-κB and IL-17, which could be targeted with specific inhibitors) and upstream regulators predicted to be inhibited.

The top five inhibited regulators included one glucocorticoid and four kinase inhibitors; these drugs may be able to directly block part of the host response and impact viral replication/pathogenesis. Among them, LY294002, a potent inhibitor of phosphatidylinositol 3 kinase (PI3K), has known antiviral activity, inhibiting the replication of influenza virus (38), vaccinia virus (39), and HCMV (40). SB203580, an inhibitor of p38 MAPK, is also an effective antiviral against the encephalomyocarditis virus (41), RSV (42), and HIV (43). LY294002 and SB203580 were also identified in Connectivity Map, a database of drug-associated gene expression profiles (22), as molecules reversing components of the HCoV-EMC gene expression signature. Finally, SB203580 showed promising antiviral results against both HCoV-EMC and SARS-CoV in our *in vitro* assay (Fig. 4C). Further extensive studies, including dose-response tests and tests of other kinases inhibitors, are ongoing. Nonetheless, these results validate our genome-based drug prediction, which allows rapid identification of effective antivirals. Despite central roles of PI3K and MAPK pathways in regulating multiple cellular processes, many kinase inhibitors targeting these pathways have been shown to be safe and well tolerated *in vivo* (reviewed in references 44 and 45). It has been hypothesized that mitogenic MAPK and survival PI3K/Akt pathways may be of major importance only during early development of an organism and may be dispensable in adult tissues (13). Several drugs targeting JNK, PI3K, and MEK have shown promising therapeutic potential in humans against a variety of diseases, including cancer and inflammatory disorder (44, 45). p38 MAPK inhibitors have also been evaluated in humans, but the first generation of molecules, including SB203580, has a high *in vivo* toxicity (liver and/or central nervous system). However, development of novel nontoxic inhibitors (e.g., ML3403) (46), more selective molecules (e.g., AS1940477) (47), and administration via inhalation (48) are promising strategies for use of this class of inhibitor for treatment of pulmonary disease. Overall, these results indicate that kinase inhibitors could be used as broad anti-CoV agents which might be combined with other host-targeting molecules, like peroxisome proliferator-activated receptor α (PPARα) agonists, to better inhibit HCoV-EMC replication.

In conclusion, using global gene expression profiling, we have shown that HCoV-EMC induces a dramatic host transcriptional response, most of which does not overlap the response induced by SARS-CoV. This study highlights the advantages of high-throughput "-omics" to globally and efficiently characterize emerging pathogens. The robust host gene expression analysis of HCoV-EMC infection provides a plethora of data to mine for further hypotheses and understanding. Host response profiles can also be used to quickly identify possible treatment strategies, and we anticipate that host transcriptional profiling will become a gen-

eral strategy for the rapid characterization of future emerging viruses.

MATERIALS AND METHODS

Cells and virus. Calu-3 2B4 cells, a clonal population of Calu-3 cells sorted for ACE2 expression, were grown in minimum essential media (MEM; Gibco) supplemented with 20% fetal bovine serum (HyClone) and 1% antibiotic antimycotic (Gibco). Viral titrations and propagation HCoV-EMC were performed in VeroE6 cells using standard methods. Human coronavirus EMC 2012 (HCoV-EMC) was received from Bart L. Haagmans (Erasmus Medical Center, Rotterdam, Netherlands) via MTA. Experiments with SARS-CoV were previously performed under the same conditions using the same cells (19).

Calu-3 cell infections. All work was performed in a biosafety level 3 (BSL3) facility supported by redundant exhaust fans, and personnel protective equipment was worn, including Tyvek suits, hoods, and HEPA-filtered powered air-purifying respirators as previously described (49). Cells were washed with phosphate-buffered saline (PBS) and inoculated with virus at an MOI of 5 or mock diluted in PBS for 40 min at 37°C. Following inoculation, cells were washed 3 times, and fresh medium was added to signify time zero. Triplicate samples of mock-infected and virus-infected Calu-3 2B4 cells were harvested between 0 and 72 hpi.

RNA isolation and microarray processing. RNA isolation from Calu-3 2B4 cells, subsequent hybridization to Agilent 4×44K human HG arrays, and processing of raw data were performed as previously described (18). We analyzed triplicates for each time postinfection except for 12 hpi, for which one replicate did not pass RNA quality control and was therefore excluded. For direct comparison with SARS-CoV-infected cells, raw data from HCoV-EMC experiments were quantile normalized together with the SARS-CoV data set (GEO series accession number GSE33267). All probes were required to meet Agilent Feature Extraction QC criteria for all replicates at least one infection time point (33,773 probes passed QC filtering). For each sample, a $\log_2$ fold change ($\log_2$ FC) value was calculated as the difference between $\log_2$ normalized data for this sample and the average of $\log_2$ normalized data for time- and data set-matched mock-infected samples.

Statistical analysis. Differential expression was determined by comparing SARS-CoV- or HCoV-EMC-infected replicates to time- and data set-matched mock-infected controls, based on a linear model fit for each probe using the R package Limma (50). Criteria for differential expression were an absolute $\log_2$ FC of 1 and a q value of <0.01 calculated using a moderated t test with subsequent Benjamini-Hochberg correction. Differentially expressed (DE) genes after HCoV-EMC infection at early times postinfection were defined as all genes DE at 0, 3, 7, or 12 hpi, and genes DE at late times postinfection were defined as all genes DE at 18 or 24 hpi. To identify genes with similar patterns of variation at early and late times postinfection, early and late signatures were intersected considering up-regulated and down-regulated genes separately and then combined to define the signature of 207 stable genes. To cluster the genes DE at late times postinfection following HCoV-EMC infection, differential expression was also calculated directly between SARS-CoV- and HCoV-EMC-infected samples using the same criteria. A comparison of similar times postinfection was performed, except for HCoV-EMC-infected samples at 18 hpi, which were compared to SARS-CoV samples at 24 hpi. HCoV-EMC samples at 24 hpi were compared with SARS samples at 24 hpi and later times postinfection (30, 36, 48, 54, 60, and 72 hpi). Genes similarly changed between HCoV-EMC and SARS-CoV (cluster I and II) were defined as genes DE by both viruses compared to their time-matched mocks and that were also not differentially changed between HCoV-EMC and SARS-CoV in at least one of the previously listed comparisons. Genes of cluster III and IV were genes DE at late times postinfection following HCoV-EMC infection that were not similarly changed between HCoV-EMC and SARS-CoV. To further cluster the genes based on their expression value after HCoV-EMC infection, $\log_2$ FC values at 18 and 24 hpi were averaged, and clusters I and III were genes with average $\log_2$ FC

values of >0, while cluster II and IV genes had average $\log_2$ FC values of <0.

Functional enrichment and upstream regulator analysis. Functional analysis of statistically significant gene expression changes was performed using Ingenuity Pathways Knowledge Base (IPA; Ingenuity Systems). For all gene set enrichment analyses, a right-tailed Fisher's exact test was used to calculate a P value determining the probability that each biological function assigned to that data set was due to chance alone. All enrichment scores were calculated in IPA using the probes that passed our QC filter as the background data set.

Upstream regulator analysis, which was used to predict regulators and infer their activation state, is based on prior knowledge of expected effects between regulators and their known target genes according to the IPA database. A z score is calculated and determines whether gene expression changes for known targets of each regulator are consistent with what is expected from the literature ($z > 2$, regulator predicted to be activated) or are anti-correlated with the literature ($z < 2$, regulator predicted to be inhibited).

Quantitative reverse transcription PCR (RT-PCR). RNA was reverse transcribed using the QuantiTect reverse transcription kit (Qiagen). The resulting cDNA samples were diluted 50×. Primer sets for SYBR green quantitative RT-PCR were designed using Primer3 (51). Primer sequences are available in Table S3 in the supplemental material. Relative gene expression in infected samples compared to that in mock-infected cells was calculated using the $2^{-\Delta\Delta C_T}$ method (52), using the *MYL6* gene as a calibrator, as the expression of *MYL6* did not significantly change in HCoV-EMC-infected cells in the microarray data.

Connectivity map. To determine whether some drugs can reverse the HCoV-EMC infection signature, we used the publicly available Connectivity Map (cmap) database (build 02) (22). Cmap is a collection of genome-wide transcriptional data from cultured human cells treated with 1,309 different compounds. We used the list of 207 DE genes that are stable after infection with HCoV-EMC. Agilent probes were mapped to Affymetrix U133A probe sets using the BioMart ID converter tool (53) in order to query the cmap database. Results were filtered based on their negative connectivity enrichment score.

Antiviral *in vitro* assay. For *in vitro* evaluation of the p38 MAPK inhibitor SB203580 (Sigma), VeroE6 cells were incubated for 4 h with the drug at 5 μM prior infection with HCoV-EMC at an MOI of 0.01 (pretreatment condition), medium was replaced during the 40-min infection, and medium containing SB203580 was added back following inoculation (54). For the posttreatment condition, cells were treated with SB203580 at 5 μM or type I IFN (100 U/ml; PBL Interferon Source) at 0 hpi following the infection inoculation.

Publically available data. Normalized matrixes and expression values can be found at https://www.systemsvirology.org/project/home/Data%20%26%20Resources/Experimental%20Metadata/HCoV-EMC%20infection%20in%20Calu-3%20cells/begin.view?. The other data set utilized was Calu-3 cells infected with SARS-CoV at MOI 5 (GSE33267).

Microarray data accession numbers. Raw microarray data have been deposited in NCBI's Gene Expression Omnibus under accession number GSE45042.

SUPPLEMENTAL MATERIAL

Supplemental material for this article may be found at http://mbio.asm.org/lookup/suppl/doi:10.1128/mBio.00165-13/-/DCSupplemental.

Table S1, DOCX file, 0.1 MB.
Table S2, DOCX file, 0.1 MB.
Table S3, DOCX file, 0.1 MB.
Data set S1, XLS file, 0.5 MB.

ACKNOWLEDGMENTS

REFERENCES

1. ProMED-mail. 20 September 2012, posting date. Novel coronavirus—Saudi Arabia: human isolate. http://www.promedmail.org/.

2. **Zaki AM, van Boheemen S, Bestebroer TM, Osterhaus AD, Fouchier RA.** 2012. Isolation of a novel coronavirus from a man with pneumonia in Saudi Arabia. N. Engl. J. Med. **367**:1814–1820.

3. **WHO.** 23 September 2012, posting date. Novel coronavirus infection in the United Kingdom. Global alert and response. http://www.who.int/csr/don/2012_09_23/en/index.html.

4. **Bermingham A, Chand MA, Brown CS, Aarons E, Tong C, Langrish C, Hoschler K, Brown K, Galiano M, Myers R, Pebody RG, Green HK, Boddington NL, Gopal R, Price N, Newsholme W, Drosten C, Fouchier RA, Zambon M.** 2012. Severe respiratory illness caused by a novel coronavirus, in a patient transferred to the United Kingdom from the Middle East, September 2012. Euro Surveill. **17**:20290.

5. **WHO.** 2013. Novel coronavirus infection---update. Global alert and response. http://www.who.int/csr/don/2013_03_23/en/index.html.

6. **WHO.** 2012. Background and summary of novel coronavirus infection—as of 30 November 2012. Global alert and response. http://www.who.int/csr/disease/coronavirus_infections/update_20121130/en/index.html

7. **Peiris JS, Yuen KY, Osterhaus AD, Stöhr K.** 2003. The severe acute respiratory syndrome. N. Engl. J. Med. **349**:2431–2441.

8. **Drosten C, Günther S, Preiser W, van der Werf S, Brodt HR, Becker S, Rabenau H, Panning M, Kolesnikova L, Fouchier RA, Berger A, Burguière AM, Cinatl J, Eickmann M, Escriou N, Grywna K, Kramme S, Manuguerra JC, Müller S, Rickerts V, Stürmer M, Vieth S, Klenk HD, Osterhaus AD, Schmitz H, Doerr HW.** 2003. Identification of a novel coronavirus in patients with severe acute respiratory syndrome. N. Engl. J. Med. **348**:1967–1976.

9. **van Boheemen S, de Graaf M, Lauber C, Bestebroer TM, Raj VS, Zaki AM, Osterhaus ADME, Haagmans BL, Gorbalenya AE, Snijder EJ, Fouchier RAM.** 2012. Genomic characterization of a newly discovered coronavirus associated with acute respiratory distress syndrome in humans. mBio **3**:e00473-12. http://dx.doi.org/10.1128/mBio.00473-12.

10. **Müller MA, Raj VS, Muth D, Meyer B, Kallies S, Smits SL, Wollny R, Bestebroer TM, Specht S, Suliman T, Zimmermann K, Binger T, Eckerle I, Tschapka M, Zaki AM, Osterhaus ADME, Fouchier RAM, Haagmans BL, Drosten C.** 2012. Human coronavirus EMC does not require the SARS-coronavirus receptor and maintains broad replicative capability in mammalian cell lines. mBio **3**:e00515-12. http://dx.doi.org/10.1128/mBio.00515-12.

11. **Raj VS, Mou H, Smits SL, Dekkers DH, Müller MA, Dijkman R, Muth D, Demmers JA, Zaki A, Fouchier RA, Thiel V, Drosten C, Rottier PJ, Osterhaus AD, Bosch BJ, Haagmans BL.** 2013. Dipeptidyl peptidase 4 is a functional receptor for the emerging human coronavirus-EMC. Nature **495**:251–254.

12. **Ren Z, Yan L, Zhang N, Guo Y, Yang C, Lou Z, Rao Z.** 2013. The newly emerged SARS-Like coronavirus HCoV-EMC also has an "Achilles' heel": current effective inhibitor targeting a 3C-like protease. Protein Cell **4**:248–250.

13. **Ludwig S.** 2011. Disruption of virus-host cell interactions and cell signaling pathways as an anti-viral approach against influenza virus infections. Biol. Chem. **392**:837–847.

14. **Josset L, Textoris J, Loriod B, Ferraris O, Moules V, Lina B, N'Guyen C, Diaz JJ, Rosa-Calatrava M.** 2010. Gene expression signature-based screening identifies new broadly effective influenza A antivirals. PLoS One **5**:e13169. http://dx.doi.org/10.1371/journal.pone.0013169.

15. **Tisoncik JR, Korth MJ, Simmons CP, Farrar J, Martin TR, Katze MG.** 2012. Into the eye of the cytokine storm. Microbiol. Mol. Biol. Rev. **76**:16–32. http://dx.doi.org/10.1128/MMBR.05015-11.

16. **Sirota M, Dudley JT, Kim J, Chiang AP, Morgan AA, Sweet-Cordero A, Sage J, Butte AJ.** 2011. Discovery and preclinical validation of drug indications using compendia of public gene expression data. Sci. Transl. Med. **3**:96ra77.

17. **Harcourt JL, Caidi H, Anderson LJ, Haynes LM.** 2011. Evaluation of the Calu-3 cell line as a model of in vitro respiratory syncytial virus infection. J. Virol. Methods **174**:144–149.

18. **Li C, Bankhead A III, Eisfeld AJ, Hatta Y, Jeng S, Chang JH, Aicher LD, Proll S, Ellis AL, Law GL, Waters KM, Neumann G, Katze MG, McWeeney S, Kawaoka Y.** 2011. Host regulatory network response to infection with highly pathogenic H5N1 avian influenza virus. J. Virol. **85**:10955–10967.

19. **Sims AC, Tilton SC, Menachery VD, Gralinski LE, Schafer A, Matzke MM, Webb-Robertson BJ, Chang J, Luna ML, Long CE, Shukla AK, Bankhead AR III, Burkett SE, Zornetzer G, Tseng CT, Metz TO, Pickles R, McWeeney S, Smith RD, Katze MG, Waters KM, Baric RS.** 2013. Release of SARS-CoV nuclear import block enhances host transcription in human lung cells. J. Virol. **87**:3885–3902

20. **Yoshikawa T, Hill TE, Yoshikawa N, Popov VL, Galindo CL, Garner HR, Peters CJ, Tseng CT.** 2010. Dynamic innate immune responses of human bronchial epithelial cells to severe acute respiratory syndrome-associated coronavirus infection. PLoS One **5**:e8729. http://dx.doi.org/10.1371/journal.pone.0008729.

21. **Maelfait J, Beyaert R.** 2012. Emerging role of ubiquitination in antiviral RIG-I signaling. Microbiol. Mol. Biol. Rev. **76**:33–45.

22. **Lamb J.** 2007. The connectivity map: a new tool for biomedical research. Nat. Rev. Cancer **7**:54–60.

23. **Perlman S, Zhao J.** 2013. Human coronavirus EMC is not the same as severe acute respiratory syndrome coronavirus. mBio **4**:e00002–13. http://dx.doi.org/10.1128/mBio.00002-13.

24. **Kindler E, Jónsdóttir HR, Muth D, Hamming OJ, Hartmann R, Rodriguez R, Geffers R, Fouchier RA, Drosten C, Müller MA, Dijkman R, Thiel V.** 2013. Efficient replication of the novel human betacoronavirus EMC on primary human epithelium highlights its zoonotic potential. mBio **4**:e00611–12. http://dx.doi.org/10.1128/mBio.00611-12.

25. **Ryzhakov G, Lai CC, Blazek K, To KW, Hussell T, Udalova I.** 2011. IL-17 boosts proinflammatory outcome of antiviral response in human cells. J. Immunol. **91**:5357–5362.

26. **Crowe CR, Chen K, Pociask DA, Alcorn JF, Krivich C, Enelow RI, Ross TM, Witztum JL, Kolls JK.** 2009. Critical role of IL-17RA in immunopathology of influenza infection. J. Immunol. **183**:5301–5310.

27. **Pappu R, Rutz S, Ouyang W.** 2012. Regulation of epithelial immunity by IL-17 family cytokines. Trends Immunol. **33**:343–349.

28. **Hewitt EW.** 2003. The MHC class I antigen presentation pathway: strategies for viral immune evasion. Immunology **110**:163–169.

29. **Hansen TH, Bouvier M.** 2009. MHC class I antigen presentation: learning from viral evasion strategies. Nat. Rev. Immunol. **9**:503–513.

30. **Hegde NR, Chevalier MS, Johnson DC.** 2003. Viral inhibition of MHC class II antigen presentation. Trends Immunol. **24**:278–285.

31. **Cunningham AC, Zhang JG, Moy JV, Ali S, Kirby JA.** 1997. A comparison of the antigen-presenting capabilities of class II MHC-expressing human lung epithelial and endothelial cells. Immunology **91**:458–463.

32. **Griffin TA, Nandi D, Cruz M, Fehling HJ, Kaer LV, Monaco JJ, Colbert RA.** 1998. Immunoproteasome assembly: cooperative incorporation of interferon gamma (IFN-gamma)-inducible subunits. J. Exp. Med. **187**:97–104.

33. **Stockman LJ, Bellamy R, Garner P.** 2006. SARS: systematic review of treatment effects. PLoS Med. **3**:e343. http://dx.doi.org/10.1371/journal.pmed.0030343.

34. **Coley W, Kehn-Hall K, Van Duyne R, Kashanchi F.** 2009. Novel HIV-1 therapeutics through targeting altered host cell pathways. Expert Opin. Biol. Ther. **9**:1369–1382. http://dx.doi.org/10.1517/14712590903257781.

35. **Ehrhardt C, Ruckle A, Hrincius ER, Haasbach E, Anhlan D, Ahmann K, Banning C, Reiling SJ, Kuhn J, Strobl S, Vitt D, Leban J, Planz O, Ludwig S.** The NF kappaB inhibitor SC75741 efficiently blocks influenza virus propagation and confers a high barrier for development of viral resistance. Cell. Microbiol., in press.

36. **Pfefferle S, Schöpf J, Kögl M, Friedel CC, Müller MA, Carbajo-Lozoya J, Stellberger T, von Dall'armi E, Herzog P, Kallies S, Niemeyer D, Ditt V, Kuri T, Züst R, Pumpor K, Hilgenfeld R, Schwarz F, Zimmer R, Steffen I, Weber F, Thiel V, Herrler G, Thiel HJ, Schwegmann-Wessels C, Pöhlmann S, Haas J, Drosten C, von Brunn A.** 2011. The SARS-coronavirus-host interactome: identification of cyclophilins as target for Pan-coronavirus inhibitors. PLoS Pathog. **7**:e1002331. http://dx.doi.org/10.1371/journal.ppat.1002331.

37. **Carbajo-Lozoya J, Müller MA, Kallies S, Thiel V, Drosten C, von Brunn A.** 2012. Replication of human coronaviruses SARS-CoV, HCoV-NL63 and HCoV-229E is inhibited by the drug FK506. Virus Res. **165**:112–117.

38. **Shin YK, Liu Q, Tikoo SK, Babiuk LA, Zhou Y.** 2007. Effect of the phosphatidylinositol 3-kinase/Akt pathway on influenza A virus propagation. J. Gen. Virol. **88:**942–950.

39. **Soares JA, Leite FG, Andrade LG, Torres AA, De Sousa LP, Barcelos LS, Teixeira MM, Ferreira PC, Kroon EG, Souto-Padrón T, Bonjardim CA.** 2009. Activation of the PI3K/Akt pathway early during vaccinia and cowpox virus infections is required for both host survival and viral replication. J. Virol. **83:**6883–6899.

40. **Johnson RA, Wang X, Ma XL, Huong SM, Huang ES.** 2001. Human cytomegalovirus Up-Regulates the phosphatidylinositol 3-kinase (PI3-K) pathway: inhibition of PI3-K activity inhibits viral replication and virus-induced signaling. J. Virol. **75:**6022–6032.

41. **Hirasawa K, Kim A, Han HS, Han J, Jun HS, Yoon JW.** 2003. Effect of p38 mitogen-activated protein kinase on the replication of encephalomyocarditis virus. J. Virol. **77:**5649–5656.

42. **Rixon HW, Brown G, Murray JT, Sugrue RJ.** 2005. The respiratory syncytial virus small hydrophobic protein is phosphorylated via a mitogen-activated protein kinase p38-dependent tyrosine kinase activity during virus infection. J. Gen. Virol. **86:**375–384.

43. **Kumar S, Orsini MJ, Lee JC, McDonnell PC, Debouck C, Young PR.** 1996. Activation of the HIV-1 long terminal repeat by cytokines and environmental stress requires an active CSBP/p38 MAP kinase. J. Biol. Chem. **271:**30864–30869.

44. **Sweeney SE, Firestein GS.** 2006. Mitogen activated protein kinase inhibitors: where are we now and where are we going? Ann. Rheum. Dis. **65**(Suppl 3):iii83–iii88.

45. **Rodon J, Dienstmann R, Serra V, Tabernero J.** 2013. Development of PI3K inhibitors: lessons learned from early clinical trials. Nat. Rev. Clin. Oncol. **10:**143–153.

46. **Munoz L, Ramsay EE, Manetsch M, Ge Q, Peifer C, Laufer S, Ammit AJ.** 2010. Novel p38 MAPK inhibitor ML3403 has potent anti-inflammatory activity in airway smooth muscle. Eur. J. Pharmacol. **635:**212–218.

47. **Terajima M, Inoue T, Magari K, Yamazaki H, Higashi Y, Mizuhara H.** 2013. Anti-inflammatory effect and selectivity profile of AS1940477, a novel and potent p38 mitogen-activated protein kinase inhibitor. Eur. J. Pharmacol. **698:**455–462.

48. **Millan DS, Bunnage ME, Burrows JL, Butcher KJ, Dodd PG, Evans TJ, Fairman DA, Hughes SJ, Kilty IC, Lemaitre A, Lewthwaite RA, Mahnke A, Mathias JP, Philip J, Smith RT, Stefaniak MH, Yeadon M, Phillips C.** 2011. Design and synthesis of inhaled p38 inhibitors for the treatment of chronic obstructive pulmonary disease. J. Med. Chem. **54:**7797–7814.

49. **Yount B, Curtis KM, Fritz EA, Hensley LE, Jahrling PB, Prentice E, Denison MR, Geisbert TW, Baric RS.** 2003. Reverse genetics with a full-length infectious cDNA of severe acute respiratory syndrome coronavirus. Proc. Natl. Acad. Sci. U. S. A. **100:**12995–13000.

50. **Smyth GK.** 2005. Limma: linear models for microarray data, p 397–420. *In* Gentleman R, Carey V, Dudoit S, Irizarry R, Huber W (ed), Bioinformatics and computational biology solutions using R and Bioconductor. Springer, New York, NY.

51. **Rozen S, Skaletsky H.** 2000. Primer3 on the WWW for general users and for biologist programmers. Methods Mol. Biol. **132:**365–386.

52. **Livak KJ, Schmittgen TD.** 2001. Analysis of relative gene expression data using real-time quantitative PCR and the 2($-$Delta delta C(T)) method. Methods **25:**402–408.

53. **Smedley D, Haider S, Ballester B, Holland R, London D, Thorisson G, Kasprzyk A.** 2009. Biomart—biological queries made easy. BMC Genomics **10:**22.

54. **Chen HH, Zhou XL, Shi YL, Yang J.** 2013. Roles of p38 MAPK and JNK in TGF-beta1-induced human alveolar epithelial to mesenchymal transition. Arch. Med. Res. **44:**93–98.